Defence Science Journal, Vol. 65, No. 4, July 2015, pp. 300-306, DOI : 10.14429/dsj.65.8353
© 2015, DESIDOC

Shape Optimisation of Curved Interconnecting Ducts

K. Srinivasan[!,#,*], V. Balamurugan[!] and S. Jayanti[#]

[!]*Combat Vehicles Research and Development Establishment, Chennai - 600 054, India*
[#]*Indian Institute of Technology Madras, Chennai - 600 036, India*
[*]*E-mail: srinivasan.k2@cvrde.drdo.in*

ABSTRACT

Practical ducting layout in process plants needs to satisfy a number of on-site constraints. The search for an optimal flow path around the obstructions is a multi-parameter problem and is computationally prohibitively expensive. In this study, authors proposed a rapid and efficient methodology for the optimal linkage of arbitrarily oriented fluid flow ducts using a single-parameter quadratic/cubic Bézier curves in two/three dimensions to describe the centreline of the curved duct. A smooth interconnecting duct can then be generated by extruding the duct face along the curve. By varying the parameter either along the angular bisector or along the axes of the ducts, a family of Bézier curves is generated. Computational fluid dynamics simulations show that the relationship between pressure drop and the adjustable parameter is a unimodal curve and the optimal connecting duct is the one which has the least pressure drop while satisfying on-site constraints can be used for linking the ducts. The efficacy of the method is demonstrated by applying it to some cases of practical interest.

Keywords: Fluid flow, ducting, shape optimisation, Bézier curves, Bernstein polynomials, computational fluid dynamics

NOMENCLATURE

B	Blending function
C_μ	Constant in the turbulence model
e, f, g	Blending functions
k	Turbulent kinetic energy
p	Pressure of the fluid
t	Time
u	Velocity
U	Time-averaged velocity
W	Duct width
x	Coordinate
ε	Rate of dissipation of turbulent kinetic energy
ρ	Density
μ	Viscosity
Subscript	
i	i^{th} control point or coordinate axis
j	Coordinate axis
k	Coordinate axis
t	Turbulent
Superscript	
$'$	Fluctuating component
n	Number of control points

1. INTRODUCTION

Optimal shape design problems have been a topic of research for a quite long time due to their application in many engineering fields. Nowadays, optimisation has become an integral step of the design process and has to cater to the needs of reducing the initial and operating costs within the restrictions in available infrastructure while meeting the requirements of process, safety and environment, etc. There has been a renewed and tremendous interest in shape optimisation in the recent years[1,2], in particular, shape optimisation of curved ducts has attracted many researchers due to their ubiquitous presence in pipe fittings, air intakes, diffusers, turbine and blade passages, cyclones, headers, etc[1-8].

The focus of the present work is on the optimisation of pipeline layout in process industries where the piping has to undergo sudden changes of direction due to on-site constraints. A simple layout can be made by providing sharp corners to go around the obstacles. A more optimal solution is one which has a gentle curvature to minimize the pressure losses. However, finding the optimal curvature is not simple due to the complicated nature of the flow through a curved duct[9,10]. While the effect of a bend in simple cases is well-understood, the flow development within the bend depends on a number of factors and general thumb rules cannot be developed to determine the curvature for minimizing the pressure drop. A methodology of design must be developed which can be used to obtain case-specific solutions taking account of the flow and geometric features of the case. In recent years, advanced flow simulation techniques incorporating computational fluid dynamics (CFD) principles are being used increasingly for the design and analysis of fluid dynamic systems[6,11]. A number of approaches have been proposed in the literature for a systematic shape optimisation of flow through curved ducts; these include

Received 13 January 2015, revised 12 July 2015, online published 30 July 2015

black-box algorithms including a multi-objective optimiser, adjoint methods for the calculation of sensitivities and topology optimisation for the optimal exploitation of available design space. These have been used to obtain optimised bend shapes involving a wide variation in cross-sectional area of the duct[5]. This may not be acceptable in a wide range of process industry applications where constraints related to on-site erection of piping necessitate maintaining nearly a constant shape of the cross-section in the bend. With this constraint, the problem of optimal linking two pipes reduces to one of finding the optimal curvature of the connecting pipe or more specifically the shape of its centreline. A number of shape parameterisation techniques and shape deformations have been proposed in the literature[2,12] including Bézier, B-spline, and non uniform rational B-spline (NURBS) curves and surfaces. As the present work is concerned with joining two pipes for smooth flow of a fluid from one to the other, it is necessary to ensure that these curves are smooth. Bézier curves possess some interesting properties which make them suitable for its use in the representation of smooth curves[13-15] and hence these are adopted in the present study for shape optimisation.

2. PROPOSED METHOD FOR LINKAGE USING BÉZIER CURVES

2.1 Bézier Curves

Bézier curves[15] are represented by a set of points known as 'control points'. The control over the variation of the shape of the curve is carried out by moving the control points which then become the design variable for controlling the shape. Extension to three dimensions is rather straight forward and can be achieved by control points located in 3-D space. A cubic Bézier curve is shown in Fig. 1. A degree *n* Bézier curve has *n+1* control points. The curve passes through the first and the last control point and is tangent to the control polygon at those end points. Thus, line segments P_0P_1 and P_2P_3 are tangents to the curve. The curve lies within the convex hull of the control points. The shape variation of the Bézier curve is obtained by the movement of the control points. For a cubic Bézier curve, a family of lines can be generated by moving points P_1 and P_2, as illustrated in Fig. 1. The equation for a Bézier curve is given by

$$P(t)=\sum_{i=0}^{i=n} B_i^n(t)P_i \quad t\in[0,1] \tag{1}$$

where the blending function $B_i^n(t)$ is given by the Bernstein polynomials

$$B_i^n(t)=\frac{n!}{(n-i)!i!}(1-t)^{n-i}\,t^i \tag{2}$$

Here P_i are the locations of the control points.

2.2 Method for Generating Family of Bézier Curves

Authors discussed the proposed method by considering the use of a Bézier curve to optimally connect two ducts resembling the shape of the alphabet *N*. The two ducts of width *W* are separated 10W apart. The length of the inlet and outlet sections is 20W each. The duct axes of the inlet and outlet sections do not intersect but overlap for a length of 10W, as shown schematically in Fig. 2(a). We seek to represent the centreline of the duct the connecting duct by a Bézier curve. Taking advantage of geometric symmetry, the Bézier curve can be defined by the three control points, namely, *A, B,* and *C* [Fig. 2(a)] where *C* is the midpoint of the line PQ and *P* is situated at half the distance of AX. Figure 2(b) shows a family of lines produced by moving point *B*. It is proposed that these smooth curves can potentially be used to describe the centreline of a curved duct which joins the inlet and the outlet ducts. For a given centreline path, the duct geometry can be obtained by extruding the inlet or outlet duct cross-section. This produces thus a curved duct linking the inlet and the outlet duct. The pressure drop for the flow through this curved can be estimated by usual CFD calculations. The process can be repeated for several of the possible Bézier curves and the best of these can be chosen. Alternatively, a formal search algorithm can be used to find the best curve.

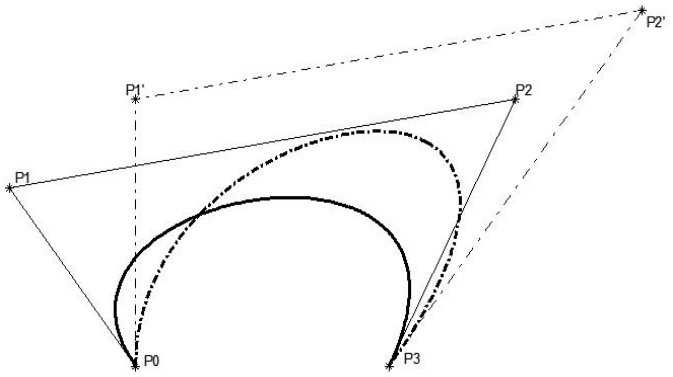

Figure 1. Two cubic Bezier curves with four control points (P_i and *Pi*) and control polygons.

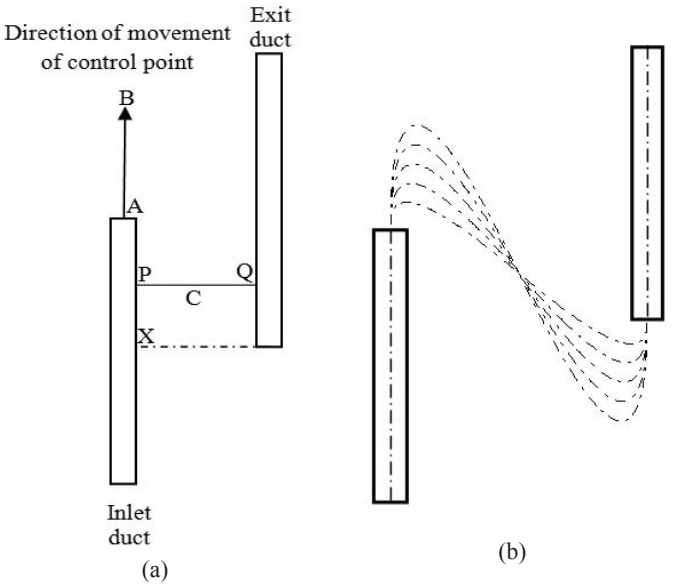

Figure 2. (a) Scheme for the generation of a family of Bezier curves for joining the two non-intersecting co-planar ducts and (b) Schematic movement of the third control point along a line to generate a family of Bezier curves linking the two pipe line segments.

As can be gathered from the above description, the method readily lends itself for automation. The principal advantage of the proposed method is that it reduces the problem of finding the optimal curvature to varying one parameter over a well-defined range, in this case, over the distance AB (Fig. 2(a)). From the known location of the control points for the optimal curve, the shape of the centreline of the connecting duct can be readily evaluated using Eqns (1) and (2). The method is quite flexible as will be shown below**.**

2.3 Solution Methodology

Finding the optimal linkage requires repetitive and fresh CFD calculation for each possible Bézier curve. Automation of this process is readily possible on commercially available CFD platforms. In the present study, the CFD code FLUENT is used for the solution of the Navier-Stokes equations (see below), the GAMBIT is used for grid generation and MATLAB is used for the generation of the centreline and for overall control using journal files that contain GAMBIT and FLUENT commands. A MATLAB code has been developed for the continuous variation of the control point to define different centreline curvatures using Bézier curves. In order to automate the entire process, MATLAB, GAMBIT and FLUENT are integrated. MATLAB interacts with GAMBIT and FLUENT via operating system through batch files and the whole calculation runs in the background[7,18]. In the present study, the numerical simulations have been carried out on a computer with Intel Core i7 processor and 8 GB RAM.

The flow field corresponding to a specific duct geometry is obtained by numerically solving the Navier Stokes equations. Using Einstein's summation convention of repeated indices, these can be written in a Cartesian coordinate system as

$$\frac{\partial \rho}{\partial t} + \frac{\partial}{\partial x_i}(\rho u_i) = 0 \tag{3}$$

$$\frac{\partial}{\partial t}(\rho u_i) + \frac{\partial}{\partial x_j}(\rho u_i u_j) = -\frac{\partial p}{\partial x_i} + \frac{\partial}{\partial x_j}\left[\mu\left(\frac{\partial u_i}{\partial x_j} + \frac{\partial u_j}{\partial x_i} - \frac{2}{3}\frac{\partial u_k}{\partial x_k}\right)\right] \tag{4}$$

Here ρ is the density, μ is the viscosity, p is the pressure and u_i is the velocity component the i^{th} direction. In case of turbulent flow, the Reynolds-Averaged Navier Stokes (RANS) equations[16] are solved. Time-averaging gives rise to Reynolds stresses, $-\rho\overline{u_i' u_j'}$, where u_i' is the fluctuating part of the i^{th} velocity component and the overbar indicates time averaging. A plethora of turbulence models are available; in the present study, the turbulent flow field is calculated using the realizable k-ε model[16]. In this case, the Reynolds stress terms are modelled through Boussinessq approach to close the equations:

$$-\rho\overline{u_i' u_j'} = \mu_t\left(\frac{\partial U_i}{\partial x_j} + \frac{\partial U_j}{\partial x_i}\right) - \frac{2}{3}(\rho k)\delta ij \tag{5}$$

where μ_i is the time-averaged value of the i^{th} velocity component, μ_t is the turbulent or eddy viscosity given by

$$\mu_t = C_\mu \frac{k^2}{\varepsilon} \tag{6}$$

The turbulent viscosity is computed by solving the transport equations for turbulent kinetic energy (k) and its rate of dissipation (ε).

3. RESULTS

3.1 Application to a Co-planar N-bend

The base case geometry of N-bend is shown in Fig. 3. The width of each duct is taken to be 0.05 m, the length is 1 m and the ducts are co-planar with an overlap region of 0.5 m with centreline to centreline separation distance of 0.5 m. The base case in which these are connected by a straight section is shown in Figure 3. The boundary conditions are as follows. On all walls, a no-slip, zero-velocity condition is applied. A uniform air velocity of 15 m/s (corresponding to a Reynolds number of 100000 based on duct width and average inlet velocity) is imposed at the inlet and zero-gauge pressure boundary condition is specified at the outlet. The geometry is discretised using 56000 cells. Second order accurate discretisation schemes have been employed and a scaled residual level of $1x10^{-5}$ for the continuity equations has been used as the convergence criterion for the iterative solution scheme. Care has been taken to ensure the wall y-plus[16] lies within the range of 30 to 100 except in some localized regions of flow recirculation where the wall y-plus is < 30.

Figure 3. Base case geometry of N-bend.

The computed solution has been used to determine the pressure drop between the exit of the inlet duct and the entrance of the outlet duct for several possible curves. Typically the pressure drop has been found to exhibit a unimodal variation with increasing distance of the control point from point *B* along the duct axis, as shown in Fig. 4(a) with the pressure drop of the optimal geometry (225 Pa) being significantly lesser than that of the base case geometry (750 Pa). The parameter value corresponding to the lowest pressure drop then defines the optimal Bézier curve, which is shown in Fig. 4(b). One can see that a smooth connecting link has been obtained for this case.

Figure 5 shows the predicted velocity contours for different cases. Figure 5(a) shows the velocity field in the optimal N-bend case. In Figs. 5(b) to 5(d), the predicted velocity in the two regions are compared for the base case, for the optimal Bézier curve case and for a non-optimal Bézier bend case. It can be seen that the sharp bend in the base gives rise to significant velocity variation in the bend regions. This is reduced to some extent by providing smoother bends, as

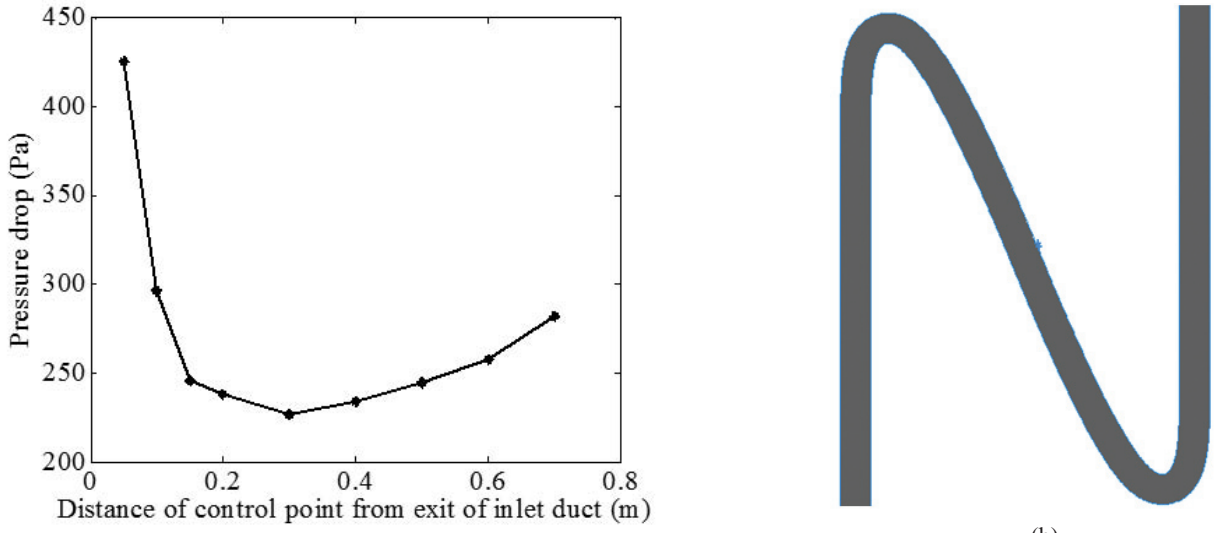

Figure 4. (a) Variation of pressure drop with respect to the location of the control points (Base case pressure drop = 750 Pa) and (b) Optimal N bend.

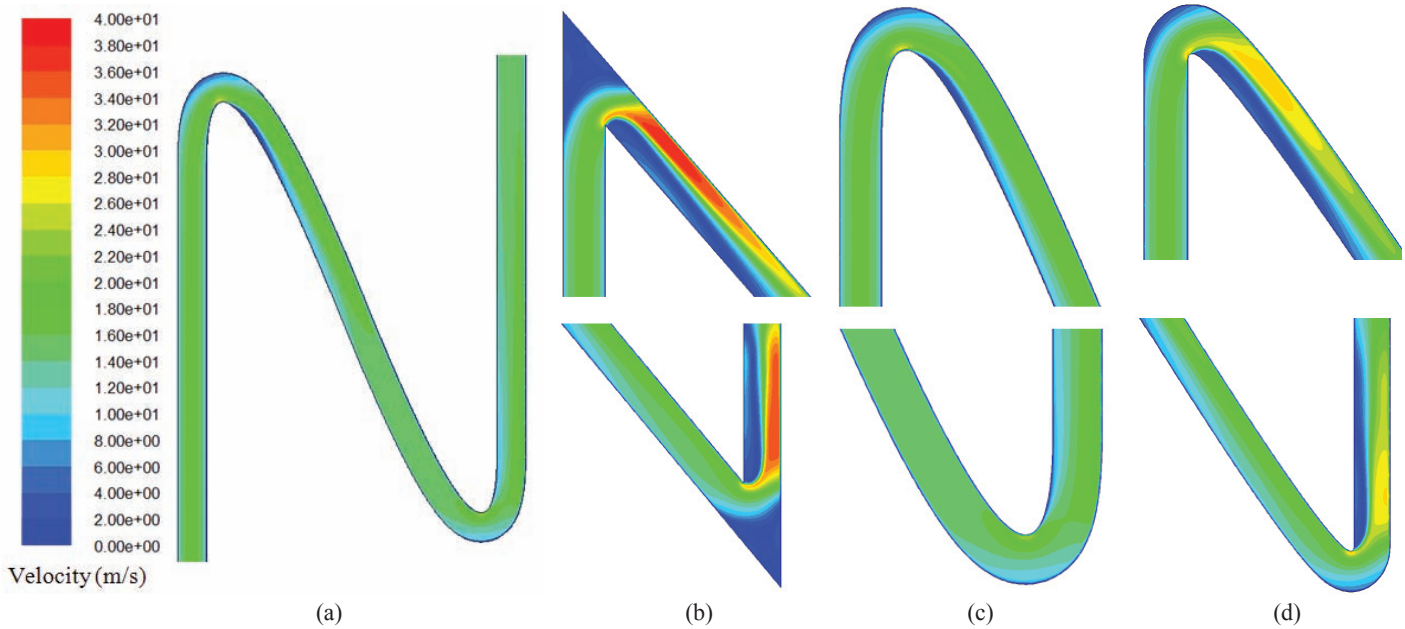

Figure 5. Velocity contours (a) in the optimal bend, and zoomed views of the velocity contours in the two bend regions for (b) the base case, (c) the optimal case and (d) a non-optimal Bezier bend case.

shown in Fig. 5(d). In the optimal bend case, which shows the least pressure drop, the velocity distribution is much more uniform throughout the domain. Thus, streamlining the flow through shape optimisation, achieved here using Bézier curves to define the centreline of the connecting duct, leads to the lowest pressure drop. The same concept is illustrated in Fig. 6 where the optimal geometries for three other co-planar bends, obtained using the same procedure, are shown.

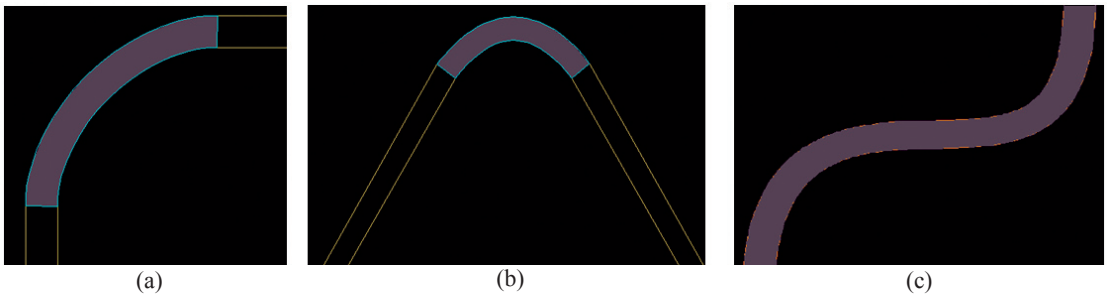

Figure 6. Predicted optimal shapes for other co-planar bend cases: (a) a 90° bend, (b) a to 60° bend, and (c) for 90° bends in tandem.

3.2 Non-coplanar Ducts

In this case, the inlet and outlet duct axes do not intersect and they do not lie in the same plane as is illustrated in Fig. 7. The connecting duct is obviously curved in three dimensions. In this case, several possible shapes for the centreline of the connecting duct can be generated by moving the two control points in the same proportion along the inlet and outlet duct axes as shown in Fig. 7(a). Considering a duct of square cross-section with a width of 0.05 m and assuming the air inlet velocity to be 30 m/s, calculations have been made for a number of possible shapes. The geometry is discretised using approximately 680,000 tetrahedral cells and three dimensional numerical simulations are performed using a duct having an inlet and outlet ducts of length 30W each, diagonal portion of the duct of length 1.732 m. The computed variation of the pressure drop between the inlet and the outlet with respect to the position of the control point is shown in Fig. 7(b). The computed 3-D path of the curved duct is shown in Fig. 8.

Compared to the base case pressure drop of 454 Pa, wherein the duct is extended along the edges of the cube until they join, one can see that the optimal case gives pressure drop of around 290 Pa. It is reiterated that the pressure drop values reported here are over the entire length of the simulated duct.

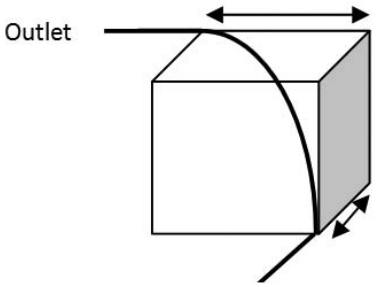

(a)

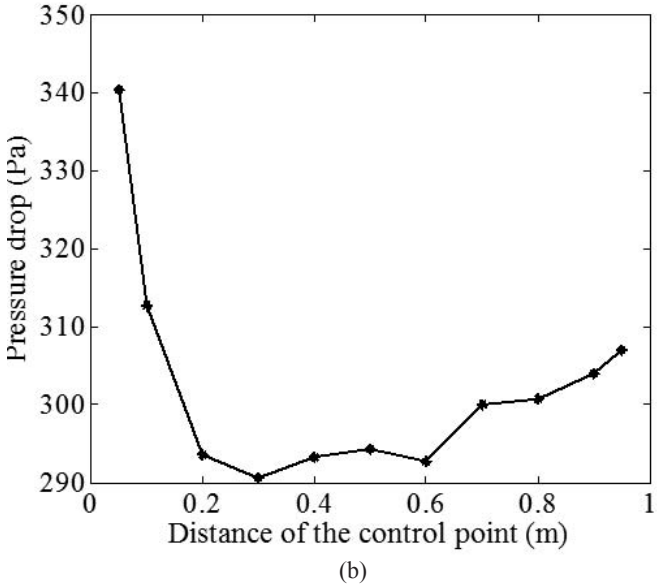

(b)

Figure 7. Application to the case of non-coplanar ducts: (a) generation of a Bezier connecting curve for a non-coplanar bend, and (b) variation of the pressure drop in the connecting duct with the location of the control point (Base case pressure drop = 454 Pa).

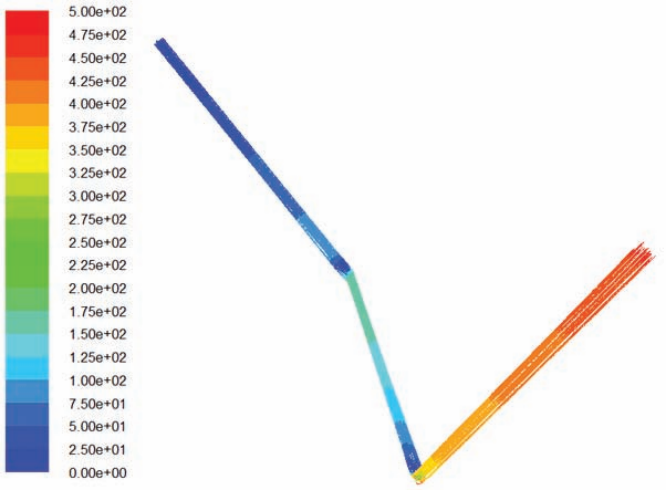

(a)

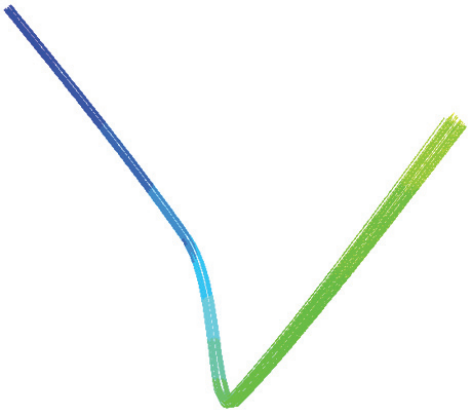

(b)

Figure 8. Pathlines coloured by static pressure (Pa) for the (a) Base case geometry, and (b) Optimal geometry.

4. MEETING ON-SITE CONSTRAINTS

When linkage of pipes separated by long distances is attempted, a number of other issues arise. Principal among these are the need to bypass existing beams and columns and the need to anchor the connecting pipe at an intermediate point. These constraints can be readily incorporated in the present method in the following way.

4.1 Bypassing Existing Columns

The presence of a beam in the pathway of the proposed connecting pipe is obviously not admissible. A pathway that largely follows the same trajectory but locally takes a detour (around the obstruction) may not be optimal from a pressure drop point of view. Given that there are several possible candidate Bézier curves joining the inlet and the outlet ducts, one should look for those curves that do not pass close to the obstruction. Consider Fig. 9(a) which shows a 3-D view of the optimal linkage for the case of non-intersecting ducts considered in section 3.2. Let us assume that there exists a column as indicated by the vertical thick black line in Fig. 9(a). The projection of the connecting pipe and the column in the x-y plane is shown in Fig. 9(b). From this, one can see that the proposed connecting line would intersect the column; this connection cannot therefore be used. Figure 9(c) shows

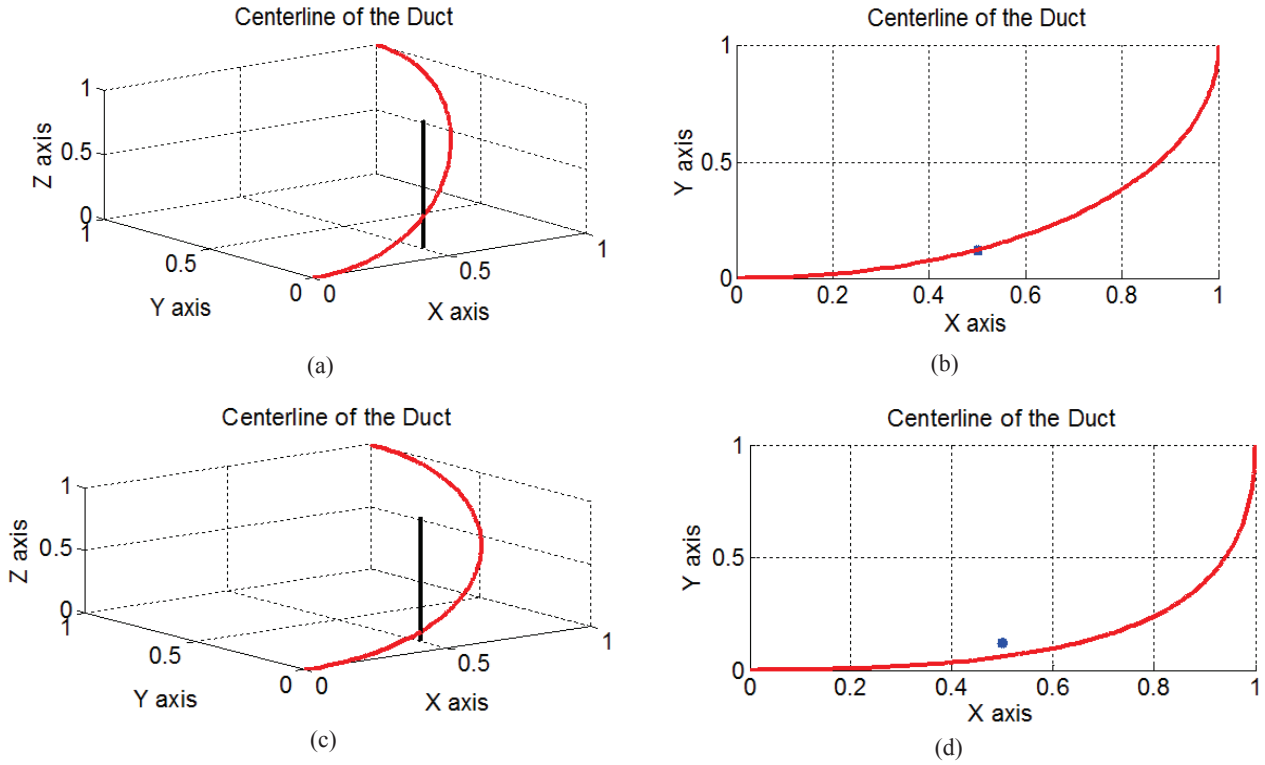

Figure 9. Meeting the constraints of existing columns in the path: (a) 3-D view and (b) and projection on the x-y plane of the centre line of the connecting pipe passing through a column, and (c) 3-D view and (d) projection of another Bezier curve connecting the same pipes but not passing through the column.

the trajectory of another Bézier curve which is close to the optimal curve. From Fig. 9(d), one can see that this curve lies at some distance from the column and is therefore not in any danger of intersecting it. Therefore, the connecting curve shown in Fig. 9(c) becomes an eligible candidate; several such eligible curves can be generated by moving the control point while ensuring that each curve is sufficiently far away from existing beams and columns through appropriate projections in the normal planes. CFD simulations of flow through these curved ducts can then be carried out to determine the one with the least pressure drop.

4.2 Providing Anchor Support

For long connecting pipes, one may wish to use an anchor support at an existing beam or column. In this case, one can look for a connecting curve which passes sufficiently close to the column using the logic described above. Alternately, one may wish to use Overhauser curves[17] in place of Bézier curves to represent the connecting duct. For example, if we wish to join two points represented by control points P_0 and P_3 smoothly but at the same time the curve need to pass through control points P_1 and P_2, then Overhauser curve is an option to do so. Overhauser curve $c(t)$ is obtained blending two quadratic curves, one passing through control points P_0, P_1 and P_2, and the other passing through control points P_1, P_2 and P_3. The Overhauser curve is defined by the following equation,

$$c(t) = f_0(t)P_0 + f_1(t)P_1 + f_2(t)P_2 + f_3(t)P_3 \; t \in [0,1] \qquad (7)$$

where $f_i(t)$ are blending functions and P_i are control points.

$$f_0(t) = -\frac{1}{2}t + t^2 - \frac{1}{2}t^3$$

$$f_1(t) = 1 - \frac{5}{2}t^2 + \frac{3}{2}t^3$$

$$f_2(t) = \frac{1}{2}t + 2t^2 - \frac{3}{2}t^3$$

$$f_3(t) = -\frac{1}{2}t^2 + \frac{1}{2}t^3$$

Figure 10 shows an Overhauser curve defined by four control points namely P_0, P_1, P_2 and P_3 where P_0 and P_3 are fixed control points and the curve is required to pass through P_1. Thus, P_2 is the only control point; by moving it along the line joining the point A and the control point P_2 (this line is perpendicular to the line joining the control points P_1 and P_2), a family of curves can be generated and the optimal link is selected from these family of curves. The optimal curve will not only be smooth and continuous, it will also pass through points P_1 and P_2 where it can be securely anchored.

5. CONCLUSION

In this paper, authors presented a rapid and efficient CFD based methodology for optimal interconnection of arbitrarily oriented fluid flow ducts which ensures streamlined flow leading to reduced pressure drop and accommodates on-site constraints such as avoiding exists beams and columns or making the duct pass close to them to provide anchor support. The method, in which the duct cross-section is maintained more

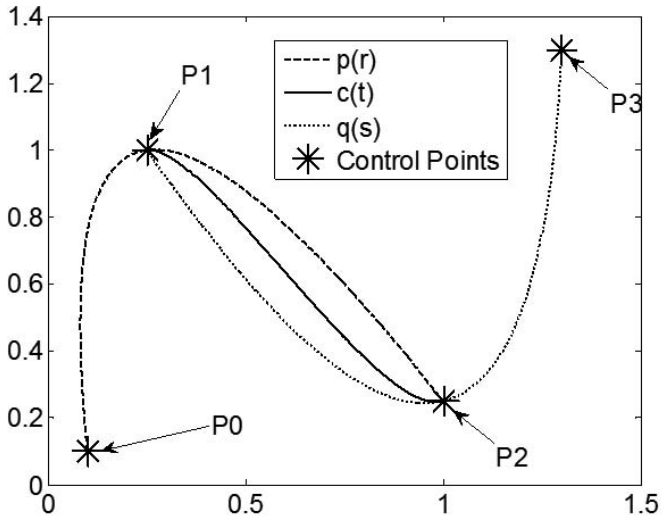

Figure 10. An Overhauser curve passing through the fixed points P_2 and P_3. By moving point P_2, a series of curves can be generated, all of which pass through the four fixed points.

or less unchanged, is posed as a single parameter optimisation problem that produces smoothly-varying centreline profile represented by a Bézier curve. The efficacy of the proposed method is successfully demonstrated using a variety of case studies. The results show that for all the candidate geometries considered, a streamlined flow is obtained in the interconnecting duct with significant reduction in the pressure drop compared to the base case.

REFERENCES

1. Pironneau, O. On optimal shapes for stokes flow. *J. Fluid Mech.* 1973, **70**(1), 331-340. doi: 10.1017/S002211207300145X
2. Kim, C. Computational elements for high-fidelity aerodynamic analysis and design optimisation. *Def. Sci. J.*, 2010, **60**(6), 628-638. doi: 10.14429/dsj.60.581
3. Jameson, A. Aerodynamic design using control theory. *J. Sci. Comput.*, 1988, **3**(3), 233-260. doi: 10.1007/BF01061285
4. Park, K.; Hong, H.; Lee, J.; Ahn, J. & Park, S. Flow control and optimal shape of headbox using CFD and SMOGA. *Int. J. Aerospace Mech. Eng.*, 2010, **4**(3), 143-148.
5. Cefarin, M.; Poloni, C. & Knight, D. Automated design optimization of a U-shaped diffuser. *In* Proceedings of the Institution of the Mechanical Engineers, Part G: J. *Aerospace Eng.*, 2011, **225**, 35-44. doi: 10.1243/09544100JAERO804
6. Safikhani, H.; Hajiloo, A. & Ranjbar, M.A. Modelling and multi-objective optimization of cyclone separators using CFD and genetic algorithms. *Comput. Chem. Eng.*, 2011, **35**(9), 1064-1071. doi: 10.1016/j.compchemeng.2010.07.017
7. Ramesh, A. & Jayanti, S. Heuristic shape optimization of gas ducting in process and power plants. *Chem. Eng. Res. Des.*, 2012, **91**(6), 999-1008. doi: 10.1016/j.cherd.2012.12.006
8. El-Sayed, K & Lacor, C. CFD modeling and multi-objective optimization of cyclone geometry using desirability function, artificial neural networks and genetic algorithms. *Appl. Math. Modelling*, 2013, **37**(8), 5680-5704. doi: 10.1016/j.apm.2012.11.010
9. Berger, S. A.; Talbot, L. & Yao, L. S. Flow in curved pipes. *Annu. Rev. Fluid Mech.*, 1983, **15**, 461-512. doi: 10.1146/annurev.fl.15.010183.002333
10. Modi, P.P. & Jayanti, S. Pressure losses and flow maldistribution in ducts with sharp bends. *Chem. Eng. Res. Des.*, 2004, **82**(3), 321-331. doi: 10.1205/026387604322870435
11. Javed, A; Manna, P. & Chakraborty, D. Numerical simulation of a dual pulse solid rocket motor flow field. *Def. Sci. J.*, 2012, **62**(6), 369-374. doi: 10.14429/dsj.62.1418
12. Samareh, J.A. A survey of shape parameterization techniques. NASA CP-1999-209136,333-343, 1999.
13. Faraway, J.J.; Reed, M.P. & Wang, J. Modelling three-dimensional trajectories by using Bézier curves with application to hand motion. *Appl. Stat.*, 2007, **56**(5), 571-85. doi: 10.1111/j.1467-9876.2007.00592.x
14. Farouki, R.T. The Bernstein polynomial basis: A centennial retrospective. *Comput. Aided Geom. Des.*, 2012, **29**(6), 379–419. doi: 10.1016/j.cagd.2012.03.001
15. Sederberg, T.W. Computer aided geometric design. Lecture Notes, Brigham Young University, 2012, Accessed on 7th July 2013 from tom.cs.byu.edu/~557/text/cagd.pd
16. Wilcox, D.C. Turbulence modelling for CFD. Griffin Printing, Glendale, 1993.
17. Brewer, J. & Anderson, D. Visual interaction with Overhauser curves and surfaces. *Computer Graphics*, 1977, **11**(2), 132-137. doi: 10.1145/965141.563883
18. Srinivasan, K. & Jayanti, S. An automated procedure for the optimal positioning of guide plates in a flow manifold using Box complex method. *Appl. Therm. Eng.*, 2015, **76**(5), 292-300. doi: 10.1016/j.applthermaleng.2014.11.015

CONTRIBUTORS

Mr K. Srinivasan is currently pursuing Ph.D. in Chemical Engineering from Indian Institute of Technology Madras, Chennai. Presently working as a Scientist at Combat Vehicles Research and Development Establishment (CVRDE), Chennai. His research interests include: Computational fluid dynamics, optimization and process control.

Dr V. Balamurugan obtained his PhD from Indian Institute of Technology Madras, Chennai. He is presently Scientist 'G' and heading Centre for Engineering Analysis and Design (CEAD) at Combat Vehicles Research and Development Estblishment (CVRDE), Chennai. His research interests include:Vibration, finite element analysis andcomputational fluid dynamics.

Dr S. Jayanti studied mechanical engineering at IIT-BHU, Varanasi, India; nuclear engineering at Ohio State University, Columbus, Ohio, USA; fluid mechanics at INPG, Grenoble, France and obtained his PhD from the Department of Chemical Engineering at Imperial College, London, UK in 1990. He is currently a professor in the department of chemical engineering at IIT Madras.His main research interests include:Computational fluid dynamics, combustion, and fuel cells.